

Provided for non-commercial research and education use.
Not for reproduction, distribution or commercial use.



This article appeared in a journal published by Elsevier. The attached copy is furnished to the author for internal non-commercial research and education use, including for instruction at the authors institution and sharing with colleagues.

Other uses, including reproduction and distribution, or selling or licensing copies, or posting to personal, institutional or third party websites are prohibited.

In most cases authors are permitted to post their version of the article (e.g. in Word or Tex form) to their personal website or institutional repository. Authors requiring further information regarding Elsevier's archiving and manuscript policies are encouraged to visit:

<http://www.elsevier.com/copyright>

Lentivirus-Based DsRed-2-Transfected Pancreatic Cancer Cells for Deep *In Vivo* Imaging of Metastatic Disease

Jiahua Zhou, M.D., Ph.D.,*¹ Zeqian Yu, M.D.,* Susu Zhao, M.D.,† Liang Hu, M.D.,* Jie Zheng, Ph.D.,†
Detong Yang, M.D.,* Michael Bouvet, M.D.,‡ and Robert M. Hoffman, Ph.D.‡§

*Department of General Surgery, Zhong Da Hospital, Southeast University, Nanjing, China; †Department of Pathology and Pathophysiology, Basic School of Medical Science, Southeast University, Nanjing, China; ‡Department of Surgery, University of California at San Diego, San Diego, California; and §AntiCancer, Inc., San Diego, California

Submitted for publication June 28, 2008

Pancreatic cancer is one of the most aggressive human malignancies. One of the leading causes of pancreatic cancer death is metastasis. In this report, we developed *in vitro*, a stable high-expression red fluorescent protein (RFP) transductant of the pancreatic cancer cells with a lentiviral expression vector containing the DsRed-2 RFP gene. These fluorescent pancreatic cancer cells were used to establish an orthotopic metastatic model and an experimental angiogenesis metastatic model of pancreatic cancer in nude mice. The high-level expression of RFP enables the imaging of distant micrometastases in their target organs. RFP expression did not interfere with the biological properties of the transformed cells compared to the parental cell line. We also demonstrated that lentiviral-transduced pancreatic cancer cells maintained stable high-level RFP expression during their growth *in vitro* and *in vivo*. The fluorescence was sufficient to noninvasively image tumor growth and metastasis, even in deep tissue such as the lung. The results indicate the benefit of lentivirus transfection of cancer cells for high expression of RFP and for sensitive *in vivo* imaging of metastatic pancreatic cancer. © 2009 Elsevier Inc. All rights reserved.

Key Words: pancreatic cancer; metastasis; micrometastasis; green fluorescent protein; red fluorescent protein.

INTRODUCTION

Pancreatic cancer is one of the most aggressive human malignancies, and approximately 37,680 new cases will be diagnosed in 2008 in the United States [1].

¹ To whom correspondence and reprint requests should be addressed at and Department of General Surgery, Zhong Da Hospital, Southeast University, Nanjing 210009, China. E-mail: zhoujh@seu.edu.cn.

Despite efforts over the past three decades to improve diagnosis and treatment, the prognosis of patients with pancreatic cancer is extremely poor with or without treatment, and no effective markers have been found for early diagnosis or effective therapy. Nearly 50% of patients have metastatic diseases at diagnosis, and nearly 100% of patients develop metastases and die of the disease. The survival rates for patients with pancreatic cancer are the lowest of all cancers; the overall 5-y survival rate is less than 4%. One of the leading causes of pancreatic cancer death is metastasis. The liver, lung, and peritoneum are the most common sites for pancreatic cancer metastasis. However, the biology of metastasis in these organs is poorly understood due to the lack of a good animal model. The cellular and molecular changes associated with cancer in animal models for human neoplastic disease are potential keys to understanding disease mechanisms. Several pancreatic cancer animal models have been established [2–5]. The early stages of tumor progression and micrometastasis formation have been difficult to analyze and have been hampered by the inability to identify small numbers of tumor cells against a background of many host cells.

The visualization of tumor cell emboli, micrometastases, and their progression over real-time during the course of the disease models has not been easy to study in current models of metastasis. Previous studies used transfection of tumor cells with the *Escherichia coli* β -galactosidase (*lacZ*) gene to detect micrometastases [6]. However, detection of *lacZ* requires extensive histological preparation; therefore, it is impossible to detect and visualize tumor cells in viable fresh tissue or the living animal at the microscopic level. Another approach for visualizing tumor cells *in vivo* involves



insertion of the luciferase gene into tumor cells causing them to emit light [7]. However, once transferred to mammalian cells, luciferase enzymes require exogenous delivery of their luciferin substrate, which is an impractical procedure in an intact animal. Because of the low resolution and signal achieved with this approach, it takes a substantial amount of time to collect sufficient photons to create a pseudo-image from an anesthetized animal. Real images cannot be displayed from the photo-counting method. Also, whether luciferase genes can function stably in tumors over long periods and in the metastases derived from them is not known.

The use of the green fluorescent protein (GFP) gene, cloned from the bioluminescent jellyfish *Aequorea victoria* [8], as a marker for localization of tumor cells in host tissues has previously been described in several studies with good results [9–11]. The tracking of cancer cells that stably express the GFP gene has been shown to facilitate *in vivo* identification of single-cell metastases and permits real-time imaging of the growth and dissemination of tumor in live animals without the use of anesthesia, contrast agents, laparotomy, or invasive procedures [12].

Red fluorescent protein (RFP) from the *Discosoma* coral possesses enhanced optical qualities that enable it to be used instead of, or as an adjunct to, GFP-based systems [13–15]. Metastatic pancreatic cancer models have been previously established by retroviral transformation of pancreatic cancer cells. Lentiviral vectors have the advantages of their ability to incorporate into genomic DNA with high efficiency, especially in cells that are not actively dividing. Lentiviral vector-mediated transgene expression can also be maintained for long periods of time. These advantages of the lentiviral vector system make it a promising new tool for establishment of transgenic animals and the manipulation of the mammalian genome. In this report, we describe a model of pancreatic cancer in which a lentivirus is used to transfect the cancer cells with RFP. We show that this model can be used for imaging tumors and metastasis at deep levels.

MATERIALS AND METHODS

Cell Lines and Culture

The SW1990 human pancreatic cancer cell line and 293 T (HEK) cells were obtained from the cell bank at the Shanghai Institute of Cell Biology, Chinese Academy of Sciences. The cells were maintained in Dulbecco's modified Eagle's medium (DMEM) supplemented with 10% heat-inactivated fetal bovine serum, 100 units/mL penicillin, and 100 μ g/mL of streptomycin, and 0.25 μ g/mL of amphotericin B (Gibco-BRL, Shanghai, China). Both cell lines were incubated at 37°C in humidified air with 5% CO₂.

Nude Mice

BALB/C $-/-$ nude mice weighing 20 to 22 g, age between 4 to 6 wk were obtained from the Experimental Animal Centre of Shanghai Slaccas. The animals were maintained in a specific pathogen-free environment. The animals were fed with an autoclaved laboratory rodent diet. The mice were maintained on a daily 12-h light–12-h dark cycle. All animal experiments involved ethical and humane treatment under a license from the Jiangsu Provincial Bureau of Science.

Lentivirus Packaging Cells

TAT-free packaging cells were used to produce recombinant lentivirus, which were obtained from the Genechem Company (Shanghai, China). The pGC-RFP plasmid together with the two packaging plasmids pHelper 1.0 [encoding human immunodeficiency virus (HIV) gag, pol, and rev] and the plasmid pHelper 2.0 [encoding for VSV-G envelope] were co-transfected into 293 T (HEK) cells using Lipofectamine 2000 (Invitrogen, Carlsbas, CA) according to the manufacturer's instructions. One day before transfection, 1.2×10^7 cells in 20 mL were plated in growth medium without antibiotics and grown to 90% to 95% confluence (in 15-cm dishes) at the time of transfection. pGC-RFP (20 μ g), plasmid pHelper 1.0 (15 μ g), and plasmid pHelper 2.0 (10 μ g) were diluted in Opti-MEM medium without serum and mixed gently (total volume 2.5 mL). Lipofectamine 2000 100 μ L was diluted in Opti-MEM medium without serum and mixed gently (total volume 2.5 mL) and incubated for 5 min at room temperature. After 5 min incubation, the diluted DNA was combined with dilute Lipofectamine 2000 (total volume is 5 mL), mixed gently, and incubated for 20 min at room temperature to permit the formation of the DNA-Lipofectamine 2000 complexes. Approximately 5 mL DNA-Lipofectamine 2000 complexes were added to each dish and mixed gently by rocking the plate back and forth. Cells were incubated in an incubator with 5% CO₂ at 37°C. After 8 h, the complexes were removed and replaced with the growth medium. The virus was harvested by collecting the cell culture medium after 48 h. After filtering the collected medium through 0.45- μ m filters, the virus was concentrated by spinning at 4000 *g* for 15 min followed by a second spin (1000 *g*, 2 min at room temperature). The concentrated virus was stored at -80°C . The titer of lentiviral vectors was determined by dilution.

RFP-Lentiviral Transduction and Selection of High RFP-Expression SW1990 Pancreatic Cancer Cells

SW1990 cells were cultured in growth medium to 30% to 50% confluence at the time of transduction (1×10^5 cells per well in 24-well plates). Then the cells were incubated with the DsRed-2 RFP-lentivirus 5 μ L (titer 5×10^8 TU/mL) for 72 h. Then, the cells were passaged at a ratio of 1:5 in selective medium that contained 400 μ g/mL G418. The level of G418 was increased to 1200 μ g/mL in a stepwise manner. High RFP-expression cell clones were selected in 96-well plates. The high RFP-expression clones were amplified and transferred by conventional culture methods.

In Vitro and *In Vivo* Growth Curves

SW1990 and SW1990-RFP cells were seeded at 1×10^5 in 60-mm culture dishes. At daily intervals, triplicate samples were harvested by trypsinization. An aliquot of 100 μ L of cell suspension was added to 100 μ L trypan blue (Sigma, St. Louis, MO) and counted using a hemocytometer. The doubling time was calculated from the cell growth curve over 5 d. To determine the *in vivo* growth potential, either 5×10^6 SW1990 and SW1990-RFP cells were injected into the flanks of nude mice. Tumor volume was measured every wk over 5 wk. Standard deviations and statistics were calculated to generate the *in vitro* and *in vivo* growth curves.

Cell Cycle Phase Distribution of Pre-and Post-Transduction of RFP

SW1990 parental cells and SW1990-RFP were cultured in DMEM supplemented with 10% heat-inactivated fetal bovine serum, 100 units/mL penicillin, 100 μ g/mL streptomycin, and 0.25 μ g/mL amphotericin B (Gibco-BRL). Cells were harvested with 0.25% trypsinization, washed thrice with cold 1% 0.01 mol/L PBS, suspended with cold 70% ethanol, and stored at -20°C . Flow cytometry analysis was then done.

Subcutaneous Tumor Growth

SW1990-RFP cells were harvested by trypsinization and washed three times with cold PBS. Approximately 5×10^6 cells were injected subcutaneously into nude mice in a total volume of 0.2 mL within 45 min of harvesting. The subcutaneous tumors were used as the source of tissue fragments for surgical orthotopic implantation (SOI) onto the pancreas as detailed below.

Surgical Orthotopic Implantation of SW1990-RFP Tumors

Orthotopic, red-fluorescent human pancreatic cancer xenografts were established in nude mice by SOI. Briefly, SW1990-RFP tumors in the exponential growth phase, grown subcutaneously in nude mice, were resected aseptically. Necrotic tissues were cut away, and the remaining healthy tumor tissues were cut with scissors and minced into 1 mm³ pieces in DMEM medium. Mice were then anesthetized with 1% pentobarbital sodium (50 mg/kg) through an abdominal cavity injection and their abdomens were sterilized with alcohol. An incision was created through the left upper abdominal pararectal line and peritoneum. The pancreas was carefully exposed and one tumor piece was transplanted onto the middle of the gland using a single 8-0 surgical suture. The pancreas was then returned into the peritoneal cavity, and the abdominal wall and the skin were closed in one layer using 6-0 surgical suture [3, 13, 16].

Tail Vein Injection

Six-week-old female nude mice were injected with 10^6 SW1990-RFP cells in the tail vein. Cells were harvested by trypsinization and washed three times with cold PBS and then injected in a total volume of 0.2 mL by using a 1-mL 29-gauge, latex-free syringe within 30 min of harvesting.

Spleen Injection

Six-week-old female nude mice were injected with 10^6 SW1990-RFP cells in the anus perineum of the spleen. Cells were harvested by trypsinization and washed three times with cold PBS and then injected in a total volume of 0.2 mL by using a 1-mL 29-gauge, latex-free syringe within 30 min of harvesting. The puncture point was impacted for 3 min with an alcohol cotton ball. Then, the abdominal wall and the skin were closed in one layer using 6-0 surgical suture.

Whole-Body Imaging

A Lighttools Research imaging system equipped with two mercury 150-W lamp power supplies was used. Selective excitation of RFP was produced through a D540/40-nm band-pass filter. Emitted fluorescence was collected through a long-pass filter (D580 nm; Chroma Technology, Rockingham, VT) on a cooled color charge-coupled-device camera. Images were processed for contrast and brightness and analyzed by Image Pro Plus 5.0 software (Media Cybernetics, Silver Spring, MD). High-resolution images of 1392×1040 pixels were captured, directly displayed on a monitor and digitally stored. Whole-body images of each mouse were obtained. At each imaging time-point,

the real-time determination of tumor burden was performed by quantifying fluorescent surface area, as previously described [14].

Internal Imaging, Analysis of Primary Tumor and Metastasis

Mice were sacrificed and explored when they appeared preorbital. Postmortem external fluorescent images were obtained. Each mouse underwent laparotomy and median sternotomy. RFP expression was visualized in the whole-body image system described above, facilitating identification of primary and metastatic pancreatic tumor. After obtaining open images, all of the solid organs were removed and were thoroughly examined for any evidence of metastasis using both fluorescence imaging and histopathological analysis.

Histopathological Analysis

Primary tumors and all organs from different models were subjected to histopathological analysis. Tumors and tissues were fixed in 10% neutral formalin at least 1 d before proceeding to paraffin embedding. Serial 4 μ m sections were cut and stained with hematoxylin and eosin for histopathological examination.

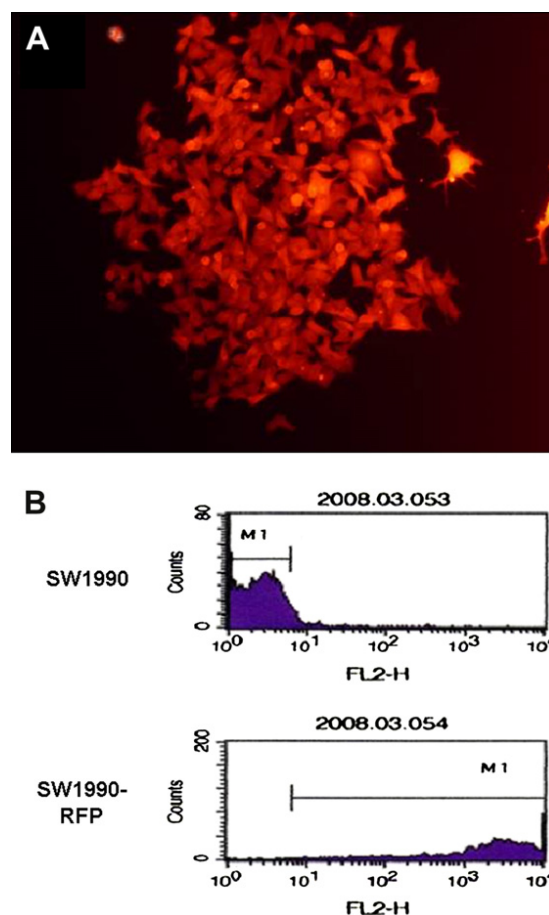


FIG. 1. Human pancreatic cancer line SW1990 was transduced by lentivirus which resulted in high-level RFP expression. (A) Strong red fluorescence was detected under fluorescence microscopy after 5 mo culture without G418 selection. (B) FACS analysis showed 99.62% RFP-expression of SW1990-RFP after 5 mo culture without G418.

RESULTS

Isolation of Stable, High-Level Expression RFP Transductants of SW1990-RFP Cells

In order to obtain fluorescent cells, SW1990 cells were transfected with the RFP-lentivirus. After transfection and selection with selective medium that contained 1200 $\mu\text{g}/\text{mL}$ G418, 70% of the resistant-colonies were fluorescent. Subclones with high RFP-expression were isolated in 96-well plates by limit dilution. A bright fluorescent clone was selected and termed SW1990-RFP (Fig. 1A). RFP-expression remained stable for 5 mo in transduced SW1990-RFP cells and could easily be monitored by fluorescence microscopy and FACS analysis of living cells (Fig. 1B), suggesting a stable chromosomal integration of the amplified RFP gene.

Effect of RFP-Expression on Biological Behavior

Experiments were carried out to determine the possible alteration of certain biological properties of SW1990-RFP compared with nontransfected SW1990 cells. No difference was observed in cell morphology and cell cycle behavior. There was no difference in the doubling-time of parental cells and selected transduced

cells as determined by comparison of proliferation in monolayer culture (Fig. 2A). Mice receiving a subcutaneous injection of SW1990 and SW1990-RFP cells were sacrificed after 6 wk. All of the mice had subcutaneous tumors. No difference in tumor size between the SW1990 and SW1990-RFP induced tumors was observed (Fig. 2B). The subcutaneous fluorescent tumor also showed parental epithelial morphology by histopathological analysis (Fig. 2C and D). These results showed that the expression of red fluorescent protein in SW1990 tumor cells does not interfere with the tumorigenicity or tumor growth *in vivo*.

Whole-Body Fluorescence Imaging of Orthotopic Primary Tumor and Metastasis

Internally growing SW1990-RFP orthotopic tumors became visible through the skin in the live animal within 10 d after implantation (Fig. 3A). The red fluorescence emitted by the tumor enabled real-time, sequential whole-body imaging and quantification of tumor burden (Fig. 3F) without the need for laparotomy, contrast agents, or invasive procedures. Orthotopically transplanted SW1990-RFP tumors produced both extensive locoregional and disseminated disease. At the time of autopsy, most of the mice had

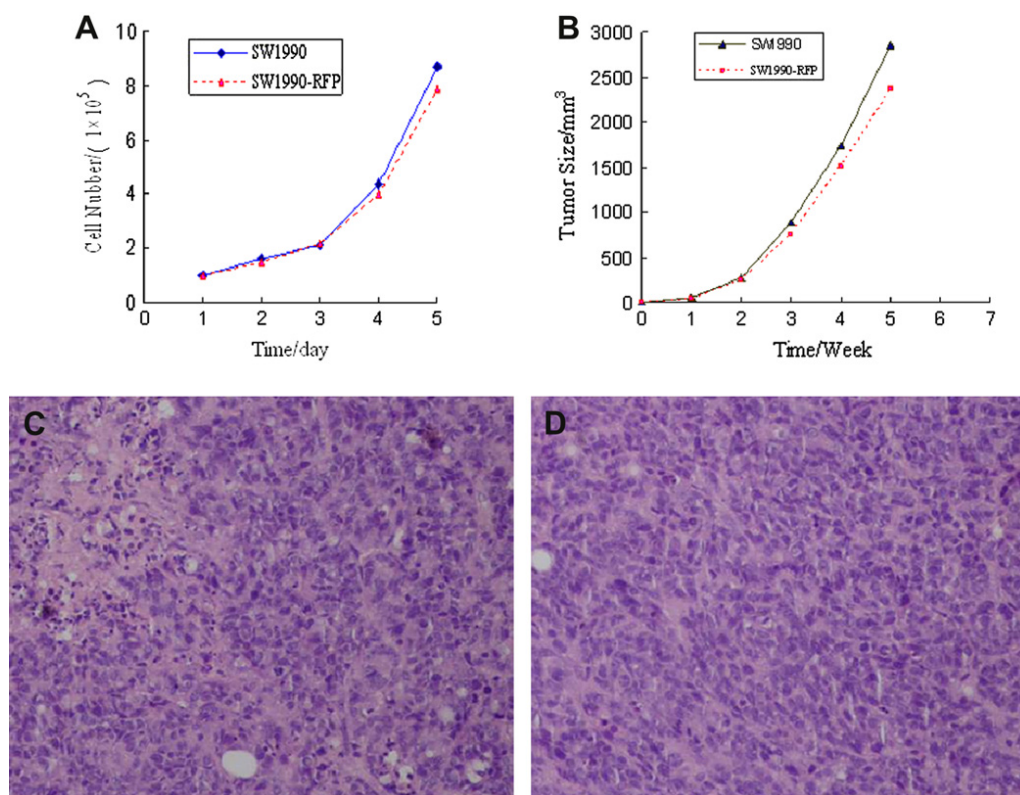


FIG. 2. Biological properties of SW1990-RFP as compared with nontransfected SW1990 cells. (A) No difference *in vitro* growth between SW1990 and SW1990-RFP was observed over 5 d. (B) No difference *in vivo* growth between SW1990 and SW1990-RFP was observed over 2 mo. (C) H&E slide of SW1990 subcutaneous tumor ($\times 200$). (D) H&E slide of SW1990-RFP subcutaneous tumor ($\times 200$).

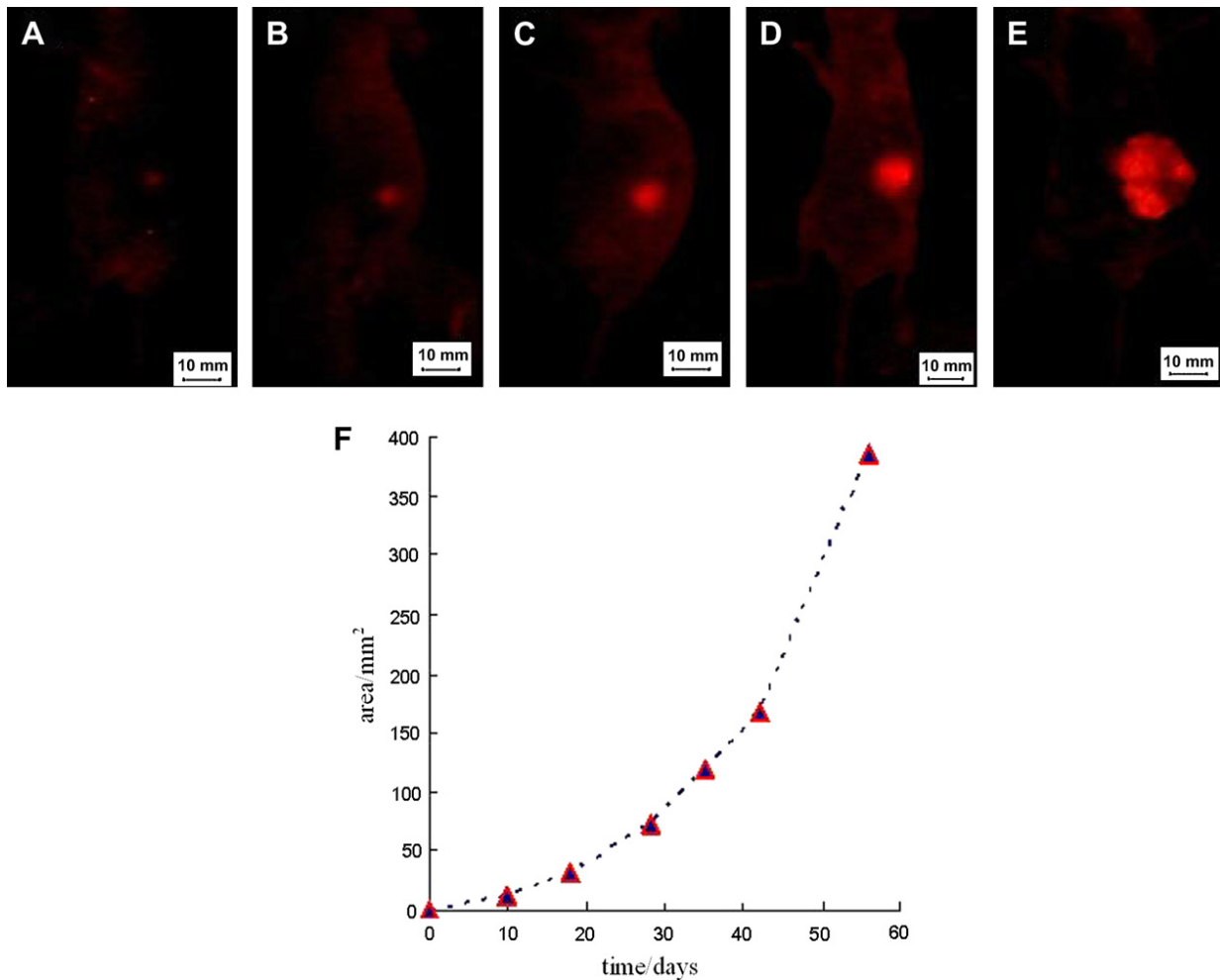


FIG. 3. RFP fluorescence enabled real-time, noninvasive *in vivo* imaging of tumor growth of SW1990-RFP tumors after surgical orthotopic implantation. (A) through (E) represent sequential fluorescent imaging of a single mouse taken on days 10, 18, 28, 35, and 56 after surgical orthotopic implantation. Progressive primary tumor growth was clearly visualized through the skin in the live animal. (F) Quantification of RFP tumor fluorescence enabled real-time quantification of total tumor burden *in vivo* after surgical orthotopic implantation.

micrometastasis and metastasis in the greater omentum, periportal lymph nodes, liver, and lung (Fig. 4). Fluorescence imaging enabled identification of micrometastases. Solid tumors were found to have histological features consistent with moderately differentiated pancreatic adenocarcinoma upon examination of hematoxylin- and eosin-stained tissue sections (Fig. 4 G).

Fluorescence Imaging of SW1990-RFP Experimental Metastases After Tail Vein Injection

Metastatic patterns of SW1990-RFP cells were also imaged after tail vein injection of 1×10^6 tumor cells into 6 nude mice. One month following tail vein injection, mice were sacrificed and explored. All the organs were observed directly under fluorescence. The location and number of metastases were recorded for each mouse. Three mice had metastasis in the lungs (Fig. 5), which were confirmed by H and E staining

(Fig. 5C). Liver metastasis was also detected in one mouse, which was also confirmed by H and E staining. No other systemic organs were involved. These results showed the lung and liver to be the preferred metastatic site for SW1990-RFP cells after tail vein injection.

Fluorescence Imaging of SW1990-RFP Experimental Metastases After Spleen Injection

Six mice were injected with SW1990-RFP in the spleen. Mice were sacrificed and explored 45 d later. All the organs were observed directly under fluorescence. Four mice were observed with many small red fluorescent tumor nodules on the surface of the liver (Fig. 6). Frozen sections expressing RFP could distinguish tumor cells and normal cells by their bright fluorescence, often down to the single-cell level (Fig 6C–E). We did not detect metastasis in other organs besides liver.

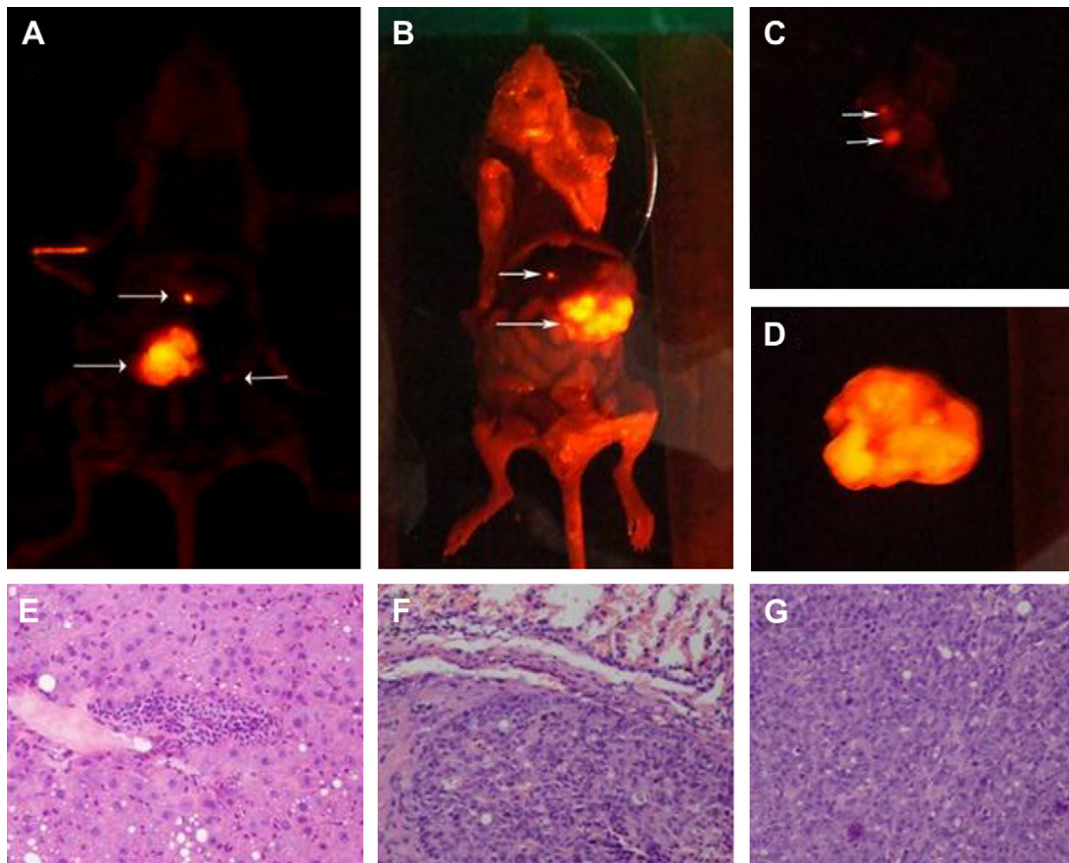


FIG. 4. Imaging of primary tumor and micrometastasis of SW1990-RFP after surgical orthotopic implantation. (A) The top arrow shows a micrometastasis of greater omentum; the middle arrows show the primary tumor and the bottom arrows show a micrometastasis of the peritoneum on day 45 after surgical orthotopic implantation. (B) The top arrows shows the micrometastasis of liver and the bottom arrow show the primary tumor taken on day 37 after surgical orthotopic implantation. (C) The two arrows show micrometastases of the lung taken on day 60 after surgical orthotopic implantation. Note, the lungs have been removed from the mouse. (D) Primary tumor emitted strong red fluorescence. (E) H&E slide of micrometastasis of liver ($\times 200$). (F) H&E slide of micrometastasis of lung ($\times 200$). (G) H&E slide of primary tumor ($\times 200$).

DISCUSSION

Medical imaging techniques have become an essential aspect of cancer diagnosis, detection, and treatment monitoring. Advances and improvements in the major imaging modalities such as ultrasonography, com-

puted tomography (CT), magnetic resonance imaging (MRI), and positron emission tomography (PET) have increased the sensitivity of visualizing tumors and their metastases in the body [17,18]. Conventional optical imaging techniques have also been severely limited by the strong absorbance and scattering of the

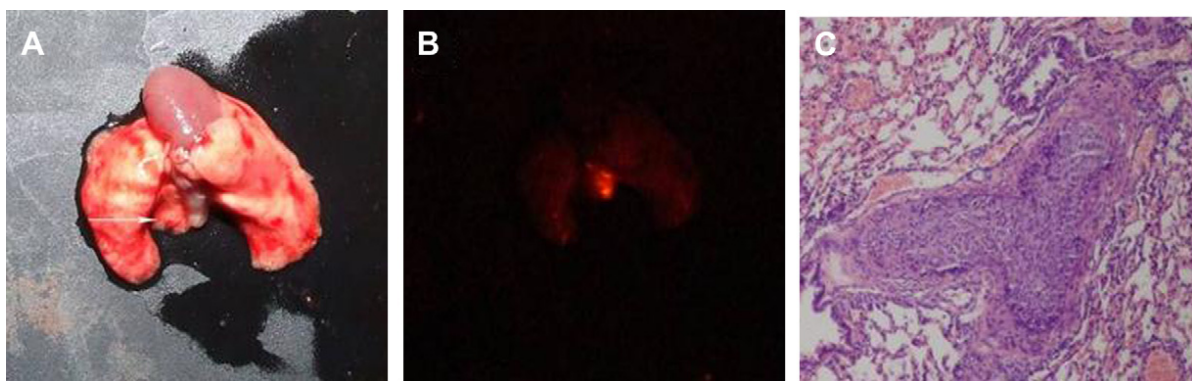


FIG. 5. Metastasis of the lung 30 d after tail vein injection. (A) Brightfield image (B) Fluorescence image lung metastasis. (C) H&E stain lung metastasis ($\times 100$).

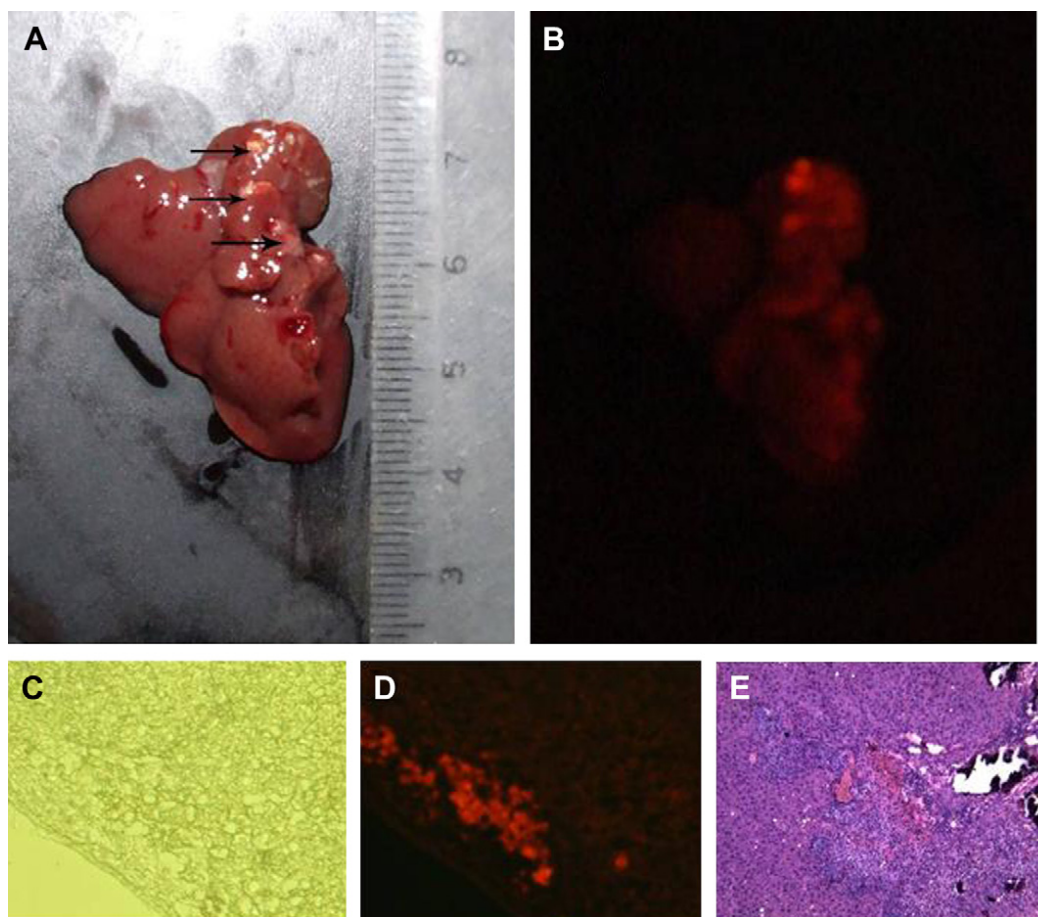


FIG. 6. Metastasis of the liver 45 d after spleen injection. (A) Brightfield image. (B) Fluorescence image. (C) Brightfield image of frozen section of liver metastasis ($\times 100$). (D) The same section as (C) observed under fluorescence microscopy ($\times 100$). (E) The H&E slide of section in (C) ($\times 100$).

illuminating light by tissue surrounding the target resulting in insufficient sensitivity and spatial resolution to image early-stage tumor growth or metastasis or inability to specifically identify malignant tissues [19]. In addition, monitoring growth and metastatic dissemination by PET, CT, or MRI is impractical because they either use potentially harmful irradiation or require harsh contrast agents and, therefore, cannot be repeated on a frequent, real-time basis. PET with the glucose analog ^{18}F -2-deoxy-D-glucose is the first molecular imaging technique that has been widely applied for cancer imaging in clinical settings [20]. Although ^{18}F -2-deoxy-D-glucose-PET has high detection sensitivity, it has limitations such as the difficulty in distinguishing between proliferating tumor cells and inflammation and the inability in using it for real-time detection of tumor tissues.

In order to attempt to improve on conventional imaging techniques, Weissleder and colleagues [21,22] infused tumor-bearing animals with probes that fluoresce at an infrared frequency when activated by protease activity. Tumors with appropriate proteases activated the probes and could be seen externally. This system is limited by

very high liver-to-tumor background fluorescence, which means that metastasis to the liver, among the most important metastatic sites, cannot be studied. Furthermore, the time limit for studies was 96 h, so growth and efficacy studies were not possible. Tumors must have appropriate protease activity to be detectable, and the probes must be delivered selectively to the tumor.

In order to externally image and follow the natural course or impediment of tumor progression and metastasis, high specificity, a strong signal, high resolution, and good physiological conditions are necessary. GFP expression in cancer cells has been shown to satisfy these criteria. In addition, tumor motility, progression, and metastasis can be visualized at the single-cell level *in vivo* with GFP [23]. RFP from the *Discosoma* coral has also been described and shown to be useful for *in vivo* imaging studies [13–15].

In the present study, RFP gene-transfected pancreatic cancer cells were successfully used to noninvasively image micrometastases of liver, omentum and peritoneum in nude mice, following surgical orthotopic implantation in the pancreas of subcutaneous tumor fragments. These models provided the opportunity to demonstrate

the capability of RFP for detection and visualization of metastases and micrometastases even in deep organs. Red-shifted RFPs are now being developed. The Katushka protein combines far-red emission and brightness, features of a fluorescent protein useful for visualization very deep within living tissues [24]. The spectral characteristics make fluorescent proteins powerful tools for cancer research, developmental biology, gene expression, and other whole-body imaging studies even in deep organs.

ACKNOWLEDGMENTS

This study was supported by the Social Development Fund of Jiangsu Province (BS2002034) and the National Natural Science Foundation (30872500).

REFERENCES

- Jemal A, Siegel R, Ward E, et al. Cancer statistics, 2008. *CA Cancer J Clin* 2008;58:71.
- Fidler IJ. Critical factors in the biology of human cancer metastasis. *Am Surg* 1995;61:1065.
- Furukawa T, Kubota T, Watanabe M, et al. A novel "patient-like" treatment model of human pancreatic cancer constructed using orthotopic transplantation of histologically intact human tumor tissue in nude mice. *Cancer Res* 1993;53:3070.
- Hotz HG, Reber HA, Hotz B, et al. An improved clinical model of orthotopic pancreatic cancer in immunocompetent Lewis rats. *Pancreas* 2001;22:113.
- Hotz HG, Reber HA, Hotz B, et al. An orthotopic nude mouse model for evaluating pathophysiology and therapy of pancreatic cancer. *Pancreas* 2003;26:e89.
- Holleran JL, Miller CJ, Culp LA. Tracking micrometastasis to multiple organs with lacZ-tagged CWR22R prostate carcinoma cells. *J Histochem Cytochem* 2000;48:643.
- Contag CH, Jenkins D, Contag PR, et al. Use of reporter genes for optical measurements of neoplastic disease in vivo. *Neoplasia* 2000;2:41.
- Prasher DC, Eckenrode VK, Ward WW, et al. Primary structure of the *Aequorea victoria* green-fluorescent protein. *Gene* 1992; 111:229.
- Hoffman RM. Green fluorescent protein imaging of tumor growth, metastasis, and angiogenesis in mouse models. *Lancet Oncol* 2002;3:546.
- Yang M, Reynoso J, Jiang P, et al. Transgenic nude mouse with ubiquitous green fluorescent protein expression as a host for human tumors. *Cancer Res* 2004;64:8651.
- Kishimoto H, Kojima T, Watanabe Y, et al. In vivo imaging of lymph node metastasis with telomerase-specific replication-selective adenovirus. *Nat Med* 2006;12:1213.
- Bouvet M, Wang J, Nardin SR, et al. Real-time optical imaging of primary tumor growth and multiple metastatic events in a pancreatic cancer orthotopic model. *Cancer Res* 2002;62:1534.
- Katz MH, Takimoto S, Spivack D, et al. A novel red fluorescent protein orthotopic pancreatic cancer model for the preclinical evaluation of chemotherapeutics. *J Surg Res* 2003;113:151.
- Katz MH, Takimoto S, Spivack D, et al. An imageable highly metastatic orthotopic red fluorescent protein model of pancreatic cancer. *Clin Exp Metastasis* 2004;21:7.
- Tsuji K, Yang M, Jiang P, et al. Common bile duct injection as a novel method for establishing red fluorescent protein (RFP)-expressing human pancreatic cancer in nude mice. *JOP* 2006; 7:193.
- Fu X, Guadagni F, Hoffman RM. A metastatic nude-mouse model of human pancreatic cancer constructed orthotopically from histologically intact patient specimens. *Proc Natl Acad Sci USA* 1992;89:5645.
- Tearney GJ, Brezinski ME, Bouma BE, et al. In vivo endoscopic optical biopsy with optical coherence tomography. *Science* 1997; 276:2037.
- MacDonald SL, Hansell DM. Staging of non-small cell lung cancer: Imaging of intrathoracic disease. *Eur J Radiol* 2003;45:18.
- Taubes G. Play of light opens a new window into the body. *Science* 1997;276:1991.
- Kelloff GJ, Hoffman JM, Johnson B, et al. Progress and promise of FDG-PET imaging for cancer patient management and oncologic drug development. *Clin Cancer Res* 2005;11:2785.
- Weissleder R, Tung CH, Mahmood U, et al. In vivo imaging of tumors with protease-activated near-infrared fluorescent probes. *Nat Biotechnol* 1999;17:375.
- Bremer C, Tung CH, Weissleder R. In vivo molecular target assessment of matrix metalloproteinase inhibition. *Nat Med* 2001;7:743.
- Chishima T, Miyagi Y, Wang X, et al. Cancer invasion and micro-metastasis visualized in live tissue by green fluorescent protein expression. *Cancer Res* 1997;57:2042.
- Shcherbo D, Merzlyak EM, Chepurnykh TV, et al. Bright far-red fluorescent protein for whole-body imaging. *Nat Methods* 2007; 4:741.